순간전압강하에 의한 단상 민감부하 및 삼상 유도전동기의 외란 민감도에 관한 연구

論 文
55A-1-7

A Study on the Susceptibility of Single-phase Sensitive Loads and the Three-phase Induction Motor by Voltage Sag

尹 尙 潤* · 文 鍾 必** · 金 載 哲† · 李 義 泰***
(Sang-Yun Yun · Jong-Fil Moon · Jae-Chul Kim · Hee-Tae Lee)

Abstract - In this paper we explore the susceptibility of common sensitive loads by voltage sags of power distribution systems. The experimental approach was used for obtaining the susceptibility of single-phase loads and the three-phase induction motor. The experimental result of single-phase loads was transformed to the ITIC(Information of Technology Industry Council) format and used for evaluating the adverse impacts of a individual and repetitive sags using the performance contour of the foreign standard data. In order to assess the impact of voltage sags on three-phase induction motor, also, the experiment was performed. The experiment was focused on the current, torque, and speed loss of the motor during a voltage sag. For comparing the impacts of individual and repetitive voltage sags, the variations of motor torque is focused among the experimental results. The sensitive curves of instantaneous current peak are used to describe the susceptibility of three-phase induction motor and also it were used for the quantitative analysis of the impact of three-phase induction motor due to voltage sags. Through the results of experiment, we verified that some types loads have more severe impact at repetitive voltage sags than individual ones and proposed method can be effectively used to evaluate the actual impact of voltage sags.

Key Words : Repetitive Voltage Sags, Susceptibility, Sensitive Loads, Three-phase Induction Motor

1. Introduction

As more electronic and precision devices are used in customer and the topology of distribution systems becomes shorter and more high-dense, both electric utilities and customers are becoming increasingly concerned about the quality of electric power. And also the power quality problems cause industrial customers to have great economic losses recently.

The power quality issues consist of two parts as a voltage quality and a frequency quality problem. The voltage sag is the most representative voltage quality problem due to the faults in power system and the temporary fault occurs more frequently than sustained interruption. Also the opposite effects is not less than the sustained interruption for the some types of customer.

Studies for assessing the impact of voltage sags on customers' load have been gradually increased. The theme of preceding approaches is primarily divided into two parts. One is the definition of voltage sag. In several standards, voltage sags are defined[1-3] and Becker et al. suggested the assumption methodology of the magnitude and the duration of voltage sag[4]. The other is the proposal of susceptibility indices for voltage sag. These methods are related to the approaches of power acceptability curves and the assessment indices. The power acceptability curves and the results of actual test for the susceptibility of voltage sags were proposed[5,6]. Conrad and Bollen presented a method to assess the effect of individual loads using the contours of the voltage sag performance[7]. The assessment index of voltage variations is proposed by Dugan and it is based on the frequency of voltage sag[8]. Lee suggest a power quality index which based on equipment sensitivity, cost, and network vulnerability[9]. Also, many studies for the voltage sag problems for three-phase induction motors were presented [10,11].

Automatic reclosing scheme has typically been employed in order to eliminate temporary faults, however it results in another unpleasant problem, the repetitive voltage sags, to the customer on the other feeders where the fault does not happen. In this paper, we explored the impact of voltage sags by experimental approach. The experimental studies of sensitive loads were carried out for obtaining the susceptibility of voltage sags and the

† 교신저자, 正會員 : 崇實大 工大 電氣工學部 敎授 · 工博
E-mail : jckim@ssu.ac.kr
* 正 會 員 : LG産電 電力硏究所 先任硏究員 · 工博
** 正 會 員 : 基礎電力硏究員 電力시스템硏究室 先任硏究員
*** 正 會 員 : 崇實大 工大 電氣工學部 博士課程
接受日字 : 2005年 8月 10日
最終完了 : 2005年 11月 14日

quantitative approaches were accomplished by using supply sag performance contours. In section 2, we summarized the evaluation methods of voltage sags using the power acceptability curves and the voltage sag coordination chart. The experimental studies for single-phase loads are presented in section 3. The results of quantitative analysis of individual and repetitive voltage sags are presented using performance contours of a foreign standard data. The experimental study for a three-phase induction motor is accomplished in section 4. The experimental results of a three-phase induction motor are transformed to the sensitivity curves of instantaneous current peak and also its effect was evaluated using the performance contour.

2. Power Acceptability Curves

Power acceptability curves have often been used to assess the impact of voltage disturbances on various customer equipment. There are two types of power acceptability curves which have been referenced very often. The most cited two curves are CBEMA(Computer Business Equipment Manufacturer Association) and ITIC(Information of Technology Industry Council) curve as shown in Fig. 1[12].

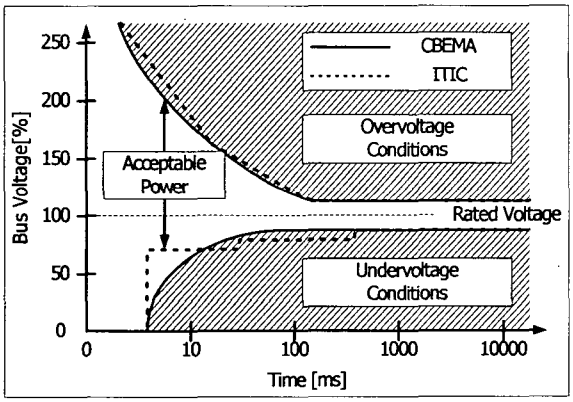

Fig. 1 Typical power acceptability curves

For the outside of the rated voltage area, two other unacceptable areas are defined in those figures. An overvoltage condition area includes the overvoltages and the voltage swells. An undervoltage condition area includes the undervoltages, the voltage sags, and the interruptions. In these unacceptable areas, customer equipment is not expected to function normally. Especially, most equipment will be severely affected in an overvoltage condition area. They might not recover to normal condition even though supply voltage recovers. Practically, ITIC curves are more useful than CBEMA curves because ITIC curve has a discrete shape unlike CBEMA curve, so it's easier to digitize than continuous CBEMA curve.

The voltage sag contours is the most representative evaluation method of voltage sag using a power acceptability curves[7]. To use this method, the contour lines should be combined that represent the stochastic data of voltage sag occurrence for a duration and a magnitude and the power acceptability curve of a load. Fig. 2 shows an example of the voltage sag contour. In Fig. 2, the oblique lines are sag contours. In this example, the voltage sag which has 400ms duration and 70% magnitude can occur X_1 times in a year. The solid and dotted lines represent the power acceptability curve for individual and successive voltage sag, respectively. The knee points of a power acceptability curve are used for calculating the number of impact of voltage sags in a year. If a equipment sensitivity is approximated by a shape with two knees as Fig. 2.

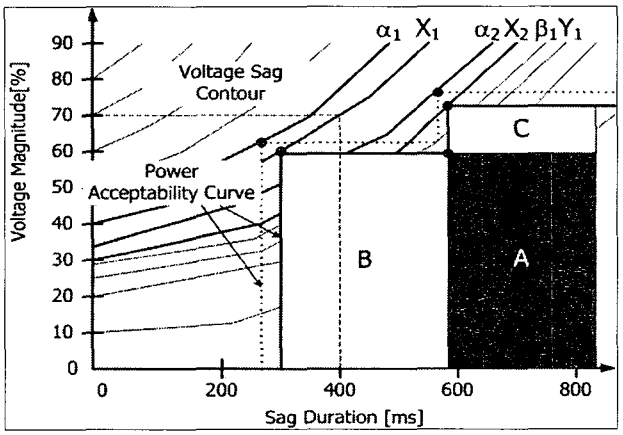

Fig. 2 Voltage sag contour and CBEMA curves

2.1 The case of especially 2 knee points

The disruption region is the combination of all three shaded rectangular areas A, B, and C. Therefore, the total number of disruption of this equipment due to the individual voltage sags is

$$N_{ID} = X_1 + X_2 - Y_1 \quad (1)$$

where, X_1 and X_2 are the number of voltage sags which intersect the knee points of non-rectangular curve, and Y_1 denotes the overlap points of two rectangular shapes. These points are related to the power acceptability curve for individual voltage sag.

2.2 The case of 2 or more knee points

If the number of knee points is N, Eq. (1) is

generally formulated as follows.

$$N_{ID} = \sum_{i=1}^{N} X_i - \sum_{i=1}^{N-1} Y_i \quad (2)$$

The coordination chart of individual voltage sag predicts N_{ID} disruptions per year for this equipment sensitivity. As shown in Fig. 2, the power acceptability curves of repetitive voltage sags are different from the curves of individual one. Therefore, the N_{RE} for the dotted line(power acceptability curve for repetitive voltage sags) is as follows.

$$N_{RE} = \sum_{i=1}^{N} \alpha_i - \sum_{i=1}^{N-1} \beta_i \quad (3)$$

where, α_i is the number of voltage sags which intersects the i-th knee points of a non-rectangular curve for a repetitive voltage sags. β_i denotes the i-th overlap points of two rectangular shapes.

2.3 The total impact of individual and repetitive voltage sag on a load

The total impact of individual and repetitive voltage sag on a load is formulated as follows.

$$N_T = (\sum_{i=1}^{N} X_i - \sum_{i=1}^{N-1} Y_i) \times P_{r1} + (\sum_{i=1}^{N} \alpha_i - \sum_{i=1}^{N-1} \beta_i) \times P_{r2} = N_{ID} P_{r1} + N_{RE} P_{r2} \quad (4)$$

where, P_{r1} is the probability of first reclosing success and P_{r2} is the probability of second reclosing attempt.

3. Impacts of Voltage Sags on Single-phase Loads

3.1 Susceptibility Analysis through Experiment

For obtaining the susceptibility of single-phase loads for repetitive voltage sags, we accomplished the actual experiment. Some single-phase loads were chosen for actual test based on [2]. The summary of test samples is shown in Table 1.

Voltage sags were generated by a three-phase source simulator(AA-2000XG). Two different procedures were tested. One was the individual impact of voltage sag and the other was performed to obtain the CBEMA curve for repetitive voltage sags. The generation time interval of repetitive voltage sags was set to be changed from 0.5s through 2s with 0.5s interval because it is typical reclosing interval which has employed in the distribution system of Korea Electric Power Corporation(KEPCO). The source simulator generated the voltage sags having magnitude varying from 10[%] to 90[%] with 10[%] interval of rated voltage. The results of the test are shown in Fig. 3. The voltage magnitude is in percent and the sag duration is in logarithmic scale of second. The CBEMA format curves in Fig. 3(a) and (b) illustrate the impact of individual and repetitive voltage sags for the automatic voltage regulator and the average values of the experiments, respectively. As shown in these figures, The cumulative impact of some loads can be found.

Table 1 Summary of actual tests

Type	Details	Confirmation of disruption
Personal computer(PC)	P-III	rebooting
Magnetic contactor(M/C)	110 and 220V	waveform
Automatic voltage regulator (AVR)	110 and 220V	waveform
High intensity discharge (HID) lamp	Metal halide	relighting
Digital power meter(DPM)	85-260V	resetting
Digital protective relay(DPR)	110 and 85-260V	resetting
Adjustable speed driver (ASD)	DC motor speed control	waveform

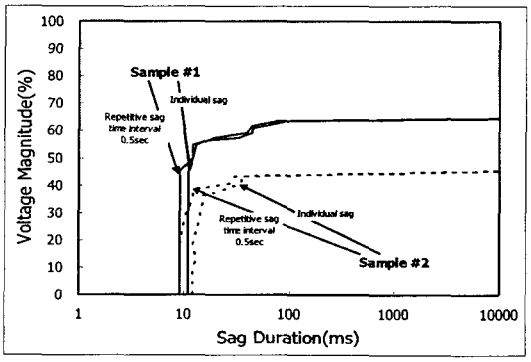

(a) Automatic voltage regulator

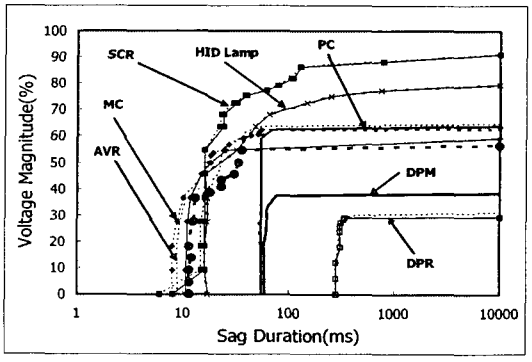

(b) Average results

Fig. 3 Test results for single phase loads

From the test results of single phase loads, SCR controller can be regarded as the most sensitive single-phase load among the tested samples. In regards to the impact of repetitive voltage sags, AVR and magnetic contactor are sensitive. It is turned out that other samples are not very affected by repetitive voltage sags.

3.2 Quantitative Analysis using Probabilistic Approach

In order to perform the quantitative analysis of the impact of voltage sag, the voltage sag coordination charts were used. Fig. 4 shows a supply sag performance contours which were derived from EPRI project[13]. We produced this contour curve using interpolation. Each contour line represents the number of occurred sags per year.

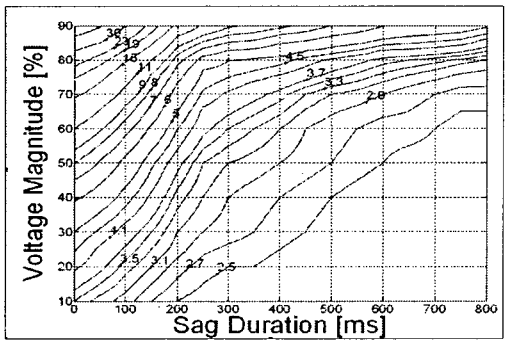

Fig. 4 Voltage sag contour from EPRI

The ITIC format curve of magnetic contactor that are derived from Fig. 4 are shown in Fig. 5. The solid lines represent individual voltage sag case and the dotted lines represent repetitive one with the generation time interval of 0.5sec. The solid line is approximated by a shape with three knees. Considered the areas shared by three knees, we can calculate the number of disruption events due to the individual voltage sags as follows. This means that there will be 8.85 process disruptions per year because of the individual voltage sags

$$N_{ID} = (8.6 + 6.9 + 5.5) - (6.7 + 5.45) = 8.85$$

Table 2 shows the number of disruption events from voltage sags for each load. That is to say, each number of the table means the possible number of disruption events from voltage sags for each load. According to the [14], it is assumed that P_{r1} and P_{r2} are 0.7(70%) and 0.3(30%), respectively. The number of disruption for individual and repetitive voltage sag, N_{ID} and N_{SU}, and the total number of the disruption due to the whole sags, N_T, are compared for each load type. The percentage of cumulative effect which compares N_{ID} with N_T is calculated as follows.

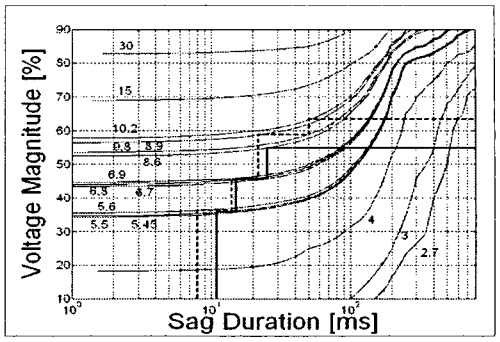

Fig. 5 Supply sag performance contours and ITIC curves for magnetic contactor

$$Cumulative\,Effect\ \% = \frac{N_T - N_{ID}}{N_{ID}} \times 100 \tag{5}$$

Table 2 Number of the disruption events for each load

Event type / Load type	N_{ID}	N_{SU}	N_T	Cumulative Effect %
PC	9.90	9.70	9.84	-0.61
M/C	8.85	11.30	9.59	8.31
AVR	8.70	11.40	9.51	9.31
HID lamp	15.40	15.50	15.43	0.19
DPM	5.00	5.10	5.03	0.60
DPR	2.76	2.78	2.77	0.22
ASD	29.70	32.30	30.48	2.63

4. Impacts of Voltage Sags on Three-phase Induction Motor

The three-phase induction motor is the common and widely used three-phase loads for an industrial plant. When a voltage sag or a short interruption takes place, the whole production process will be disrupted, many induction motors will probably be disconnected, and may not be able to accelerate its load on the restoration of the supply voltage to normal. In this paper, the influence of the motor protective equipment is neglected. The influence of induction motor for voltage sag is summarized as follows

A voltage sag will reduce the motor torque proportional to the square of the motor terminal voltage. Motor slip will increase with an increase in the line current. If we assume again that low-inertia constant torque loads are connected to the induction motor, the motor will slow down considerably and the continuity of the output may be lost. Unloading loads like pumps, compressors and fan dampers might not recover the state of the normal start

up [15]. A rapidly decaying transient torque, which has a negative peak of about five times the per-unit torque, will be produced. Current peaks will be approaching about ten times the per-unit current [15]. These transient phenomena will stress the insulation of the motor, the shaft, and the foundation.

In order to assess the impact of the voltage sags on three-phase induction motor, the experiment was performed with various points of view. Especially, we focused on the assessment of current, torque, and speed loss of the motor. Finally sensitivity curves of instantaneous current peak are produced.

We used a small three-phase squirrel-cage induction motor having following ratings: 1/3[hp], 220[V], 60[Hz], 1800[rpm]. In order to adjust the load of the motor, a small dynamometer was used in this experiment. Voltage sags were generated through a three-phase source simulator. Voltages, currents, and dynamometer's emf(electromotive force) were measured and recorded by a four-channel digital oscilloscope.

Fig. 6 shows the comprehensive flow diagram of this experiment. We divided this experiment into two categories: first, to look into no-load motor, and secondly, to conduct with a 85[%] rated motor load as connecting a dynamometer. One of the channels of the oscilloscope is used to measure the dynamometer's emf since emf can be expressed as a function of the motor speed. Thus we can check out the variation of the motor speed by monitoring emf.

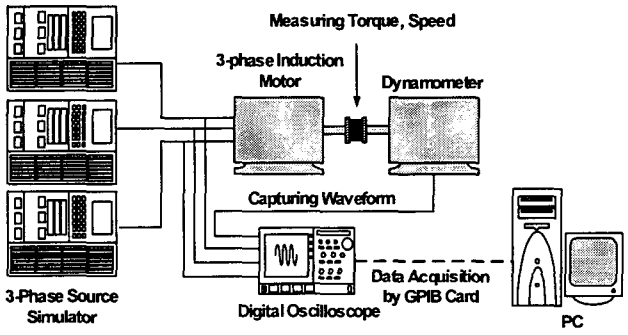

Fig. 6 Configuration of the experiment

In regards to the sag type, experiments can be divided into two parts as shown in Fig. 7; experiment for individual voltage sags and for repetitive ones. The voltage durations were set to be varied from 25 to 200ms. In the case of the repetitive voltage sag, we had the motor supplied the normal voltage for 0.5sec until the second sag began. Table 3 shows all cases taken up in this experiment and there are only no-load cases in individual events(case 1 through 3). In each case, the source simulator generated the voltage sags having the magnitude varying from 10 to 90[%] with a 10[%] interval of normal voltage. Fig. 8 shows the photo of the real configuration of the three-phase induction motor experiment.

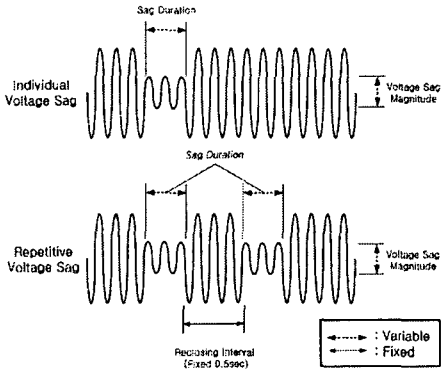

Fig. 7 Generation of individual and repetitive voltage sags

Table 3 Experiment cases of the induction motor

Case	No. of induced sags	Load rating[%]	Voltage magnitude [%]	Sag duration [ms]
Case1	1 (Individual)	No-load	0~90 Variable	25 50 75 100 150 200
Case2				
Case3				
Case4		85		
Case5				
Case6				
Case7	2 (Repetitive)	85		
Case8				
Case9				

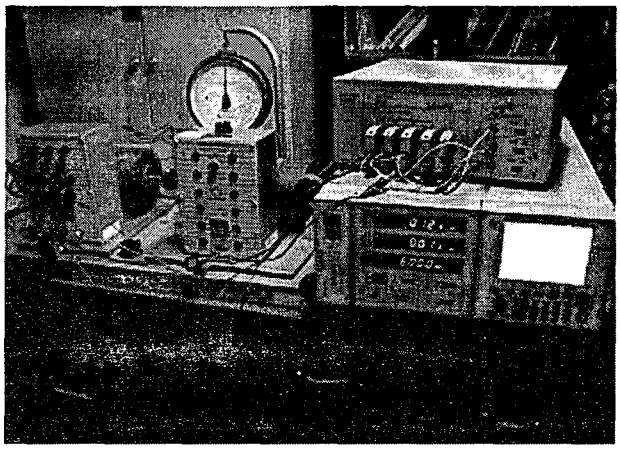

Fig. 8 Photo of the experiment of the induction motor

Fig. 9 shows the selected motor speed variation for the motor with no-load and 85[%] load during the individual event in each voltage sag depth. The range of speed reduction of 85[%] rated motor load cases is much wider than no-load cases.

Motor torque variations for repetitive voltage sags are illustrated in Fig 10. As we can see on Fig. 10, the second voltage sag may explicitly cause the torque reduction more considerably than the first ones.

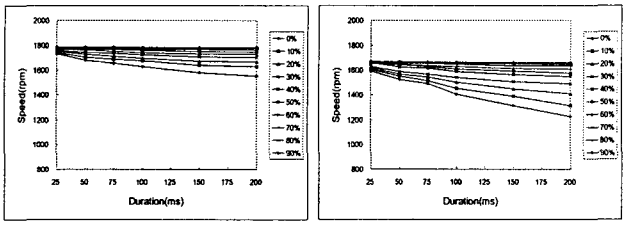

(a) single phase sag in no-load and 85% load

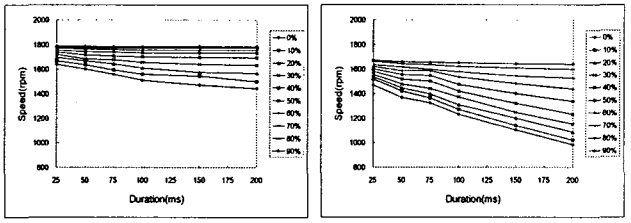

(b) three phase sag in no-load and 85% load

Fig. 9 Variations of the motor speed for no-load and 85% load(individual sag)

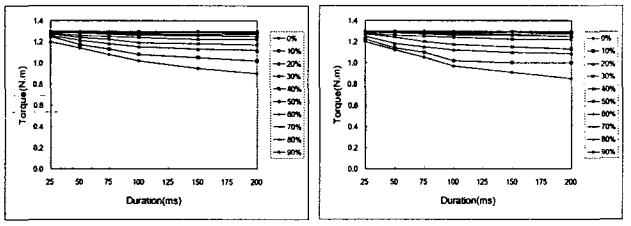

(a) single phase in individual sag and repetitive sag

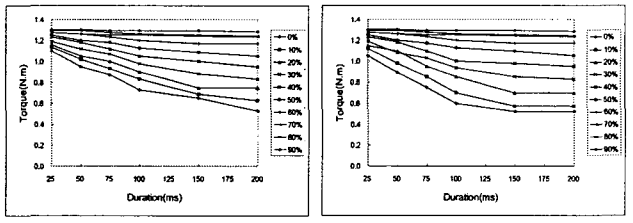

(b) three phase in individual sag and repetitive sag

Fig. 10. Variations of motor torque for repetitive voltage sags in 85% load

It is positively necessary to get the power acceptability curve of motor, which can make the quantitative assessment of voltage sag. However, it is hard to decide when and how motor meets the miss operation or malfunction because of the inertia on rotate, which is different to normal loads. Therefore, we need another parameter except magnitude and duration of voltage sag which is the variable of power acceptability curve. In this paper, the instantaneous current peak(ICP) rather than the torque peak and speed loss would be only considered because increased current would stress the insulation of the motor [12]. We derived these sensitivity curves of the ICP for a three-phase induction motor from the experimental results that we had already gotten. The values for each point of ICP are calculated in per-unit by equation (3) [18].

$$i_{peak,pu} = \frac{i_{peak}}{\sqrt{2}I_r} = \frac{\max(|i_a(t)|,\ |i_b(t)|,\ |i_c(t)|)}{\sqrt{2}I_r} \tag{6}$$

where I_r denotes the rated current of the motor and i_a, i_b and i_c are the instant current value of phase A, B and C respectively. Fig. 11 show the selected induction motor's sensitivity curves of ICP for a no-load motor and a 85[%] rated motor load, respectively. The axes of these plots represent the voltage magnitude in percent value and the duration in millisecond. Each plot consists of several level curves of ICP. These curves are similar to above power acceptability curve, which has one difference that shows the magnitude of peak current of motor by voltage sag. For example, Fig. 11(a) consists of seven number of level curves of ICP. Each line means that the ICP n times as large as the rated current occurred by the voltage sag having the magnitude and the duration correspond to sensitivity curve. where n is the one of the number, 2 to 8 at the figure.

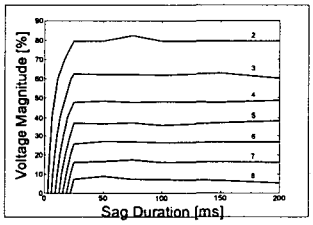

(a) no-load(single phase)

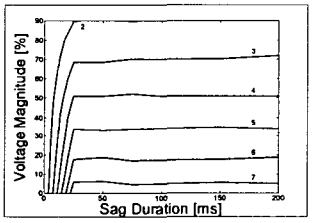

(b) 85% load(single phase)

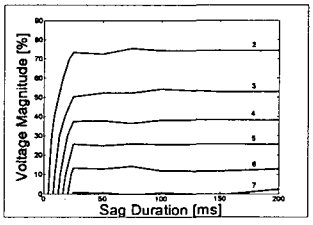

(c) no-load(double phase)

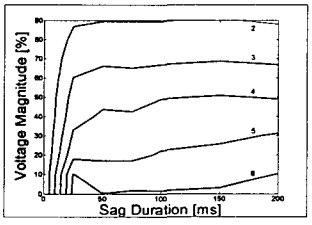

(d) 85% load(double phase)

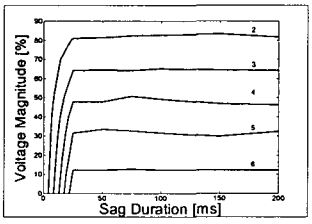

(e) no-load(three phase)

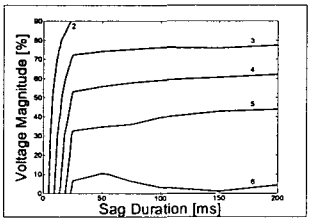

(f) 85% load(three phase)

Fig. 11 Sensitivity curves of instantaneous current peak (individual voltage sag for no-load motor)

In a case of motor load, the quantitative analysis of the impact of voltage sag was performed using the voltage sag coordination charts of Fig. 4 which like a case of single-phase load. Fig. 12 shows the voltage sag coordination chart of Fig. 4 which is applied to Fig. 11(a) and Fig. 11(b).

Table 4 shows the number of occurred ICP at three-phase induction motor by voltage sags for each case. Each cell means the number of event per year. For example, the current having 3 times of ICP of rated current occurs 10.3 per year by two-phase sag on induction motor with 85% load

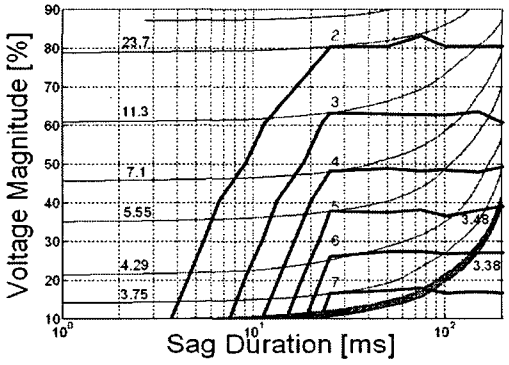

(a) No-load motor

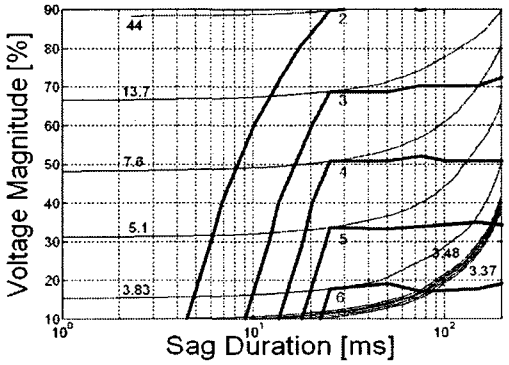

(b) 85% load motor

Fig. 12 Supply sag performance contours and instantaneous current peak sensitivity curves for single-phase voltage sag

Table 4 Number of occurred instantaneous current peak per year

Case \ ICP [p.u]		2	3	4	5	6	7
No load	Single phase sag	23.7	11.3	7.1	5.55	4.29	3.75
	Two phase sag	17	7.6	5.53	4.3	3.54	
	Three phase sag	25.7	11.8	7.1	4.9	3.5	
85% load	Single phase sag	44	13.7	7.6	5.1	3.83	
	Two phase sag	38	10.3	5	3.83		
	Three phase sag	45	16	8.9	5		

5. Conclusions

In this paper, the individual and repetitive impact of voltage sags was presented. The actual experiments for sensitive loads were accomplished to obtain the susceptibility of voltage sags. The experiment for three-phase induction motor was also conducted.

In the experiment of single-phase loads, the cumulative effect of the voltage sags was compared with individual one using voltage sag contours. It turns out that these assessment method using sag coordination chart are very effective to the voltage sag analysis. An experimental study was performed to confirm such impact on three-phase induction motor including the impact of repetitive voltage sags. From the test results, two-phase and three-phase voltage sags can be regarded as by far the worst case in regards to the motor stability. Moreover it is obvious that the repetitive voltage sags will affect the motors adversely. And also this study propose the quantitative assessment of voltage sag that make coordination chart is applied to current peak chart of motor, which prove effectiveness throughout case study.

Through the results of experiment, we verified that some types loads have a different impact between individual and repetitive voltage sags and proposed method can be effectively used to evaluate the actual impact of repetitive voltage sags. As a matter of fact, it is hard to apply these experimental results and quantitative analysis in this paper directly to other equipment but it can be applied to the basic research materials of the field of voltage quality studies.

Acknowledgement

This work has been supported by KESRI (02-jung-03), which is funded by MOCIE(Ministry of commerce, industry and energy)

References

[1] IEEE recommended practice for monitoring electric power quality, IEEE Std. 1159, 1995.

[2] IEEE guide for service to equipment sensitive to momentary voltage disturbances, IEEE Std. 1250, 1995.

[3] Electromagnetic compatibility (EMC), Part 2: Environment, Section 2: Voltage dips, short interruptions and statistical measurement results, IEC61000-2-8.

[4] C. Becker et al., "Proposed chapter9 for predicting voltage sags (dip) in revision to IEEE Std 493, the Gold Book," IEEE Trans. on Ind. Appl., vol. 30, no.

3, pp. 805-821, May/Jun. 1994.
[5] Y. Sekine, T. Yamamoto, S. Mori, N. Saito, and H. Kurokawa, "Present state momentary voltage dip interferences and the countermeasures in Japan," Int. Conf. on Large Electric Networks (CIGRE), 34th Session, Sep. 1992.
[6] J. Lamoree, D. Mueller, P. Vinett, W. Jones, and M. Samotyj, "Voltage sag analysis case studies, " IEEE Trans. on Ind. Appl., vol. 30, no. 4, pp. 1083-1089, Jul./Aug. 1994.
[7] L. E. Conrad and Math H. J. Bollen, "Voltage sag coordination for reliable plant operation," IEEE Trans. on Ind. Appl., vol. 33, no. 6, pp. 1459-1464, Nov./Dec. 1997.
[8] R. C. Dugan, D. L. Brooks, M. Waclawiak, and A. Sundaram, "Indices for assessing utility distribution system RMS variation performance," IEEE Trans. on PWRD, vol. 13, no. 1, pp. 254-259, Jan. 1998.
[9] G.-J. Lee, M. M. Albu, G. T. Heydt, "A power quality index based on equipment sensitive, cost, and network vulnerability", IEEE Trans. on PWRD, vol. 19, no. 3, pp. 1504-1510, Jul. 2004.
[10] J. C. Gomez, M. M. Morcos, C. A. Reineri, and G. N. Campetelli, "Behavior of induction motor due to voltage sags and short interruptions," IEEE Trans. on PWRD, vol. 17, no. 2, Apr. 2002.
[11] L. Guasch, F. Corcoles, J. Pedra, "Effects of symmetrical and unsymmetrical voltage sags on induction machines", IEEE Trans. on PWRD, vol. 19, no. 2, Apr. 2004.
[12] Math H. J. Bollen, Understanding power quality problems-voltage sags and interruptions, New York: IEEE Press, 2000.
[13] IEEE recommended practice for evaluating electric power system compatibility with electronic process equipment, IEEE Std. 1346, 1998.
[14] J. F. Moon, J. C. Kim, S, Y. Yun, B. S. Kang, "Quantitative Evaluation of the Impact of Low-Voltage Loads Due to the Successive Voltage Sags", Trans. on KIEE, vol. 53A, no. 12, Dec. 2004.
[15] J. C. Das, "Effects of momentary voltage dips on the operation of induction and synchronous motors", IEEE Trans. on Ind. Appl., vol. 26, no. 4, July/August, 1990.

저 자 소 개

윤 상 윤 (尹 尙 潤)

1970년 8월 28일생. 1996년 숭실대 전기공학과 졸업. 2002년 동 대학원 전기공학과 졸업(공박). 현재 LG산전 전력연구소 선임연구원.

Tel : 043-261-6506
Fax : 043-261-6629
E-mail : syyun@lsis.biz

문 종 필 (文 鍾 必)

1977년 5월 27일생. 2000년 숭실대 전기공학과 졸업. 2004년 동 대학원 전기공학과 박사 수료. 현재 기초전력연구원 선임연구원.

Tel : 02-880-7587
Fax : 02-883-0827
E-mail : pichard@snu.ac.kr

김 재 철 (金 載 哲)

1955년 7월 12일 생. 1979년 숭실대 전기공학과 졸업. 1987년 서울대 대학원 전기공학과 졸업(공학박사). 현재 숭실대 전기공학부 교수.

Tel : 02-820-0647
Fax : 02-817-0780
E-mail : jckim@ssu.ac.kr

이 희 태 (李 義 泰)

1976년 4월 2일생. 2002년 숭실대 전기공학과 졸업. 2004년 동 대학원 전기공학과 졸업(석사). 현재 동 대학원 박사과정.

Tel : 02-824-2416
Fax : 02-817-0780
E-mail : visir@ssu.ac.kr